

1 PREPARED FOR SUBMISSION TO JINST  
2 23<sup>RD</sup> INTERNATIONAL WORKSHOP ON RADIATION IMAGING DETECTORS  
3 26 - 30 JUNE 2022  
4 RIVA DEL GARDA, ITALY

## 5 Test of ITk 3D sensor pre-production modules with 6 ITkPixV1.1 chip

---

7 **F. Crescioli,<sup>a</sup> G.-F. Dalla Betta,<sup>b,c</sup> G. Gariano,<sup>d</sup> C. Gemme,<sup>d</sup> F. Guescini,<sup>e</sup> S. Hadzic,<sup>e</sup>**  
8 **T. Heim,<sup>f</sup> A. Lapertosa,<sup>d,g,1</sup> S. Ravera,<sup>d,g</sup> A. Rummler,<sup>h</sup> L. Vannoli,<sup>d,g</sup> Md. A. A. Samy,<sup>b,c</sup>**  
9 **D M S Sultan,<sup>b,c</sup> H. Ye<sup>i</sup>**

10 <sup>a</sup>*Laboratoire de Physique Nucléaire et de Hautes Energies (LPNHE), Sorbonne Université, Université Paris*  
11 *Cité, Paris, France*

12 <sup>b</sup>*Department of Industrial Engineering, University of Trento, Trento, Italy*

13 <sup>c</sup>*TIFPA INFN, Trento, Italy*

14 <sup>d</sup>*INFN Genoa, Genoa, Italy*

15 <sup>e</sup>*Max-Planck-Institut für Physik, Munich, Germany*

16 <sup>f</sup>*Lawrence Berkeley National Laboratory and University of California, Berkeley, USA*

17 <sup>g</sup>*Department of Physics, University of Genoa, Genoa, Italy*

18 <sup>h</sup>*European Laboratory for Particle Physics, CERN*

19 <sup>i</sup>*Georg-August-Universität Goettingen, II. Physikalisches Institut, Goettingen, Germany*

20 *E-mail: [alessandro.lapertosa@cern.ch](mailto:alessandro.lapertosa@cern.ch)*

21 **ABSTRACT:** ITk detector, the new ATLAS tracking system at High Luminosity LHC, will be equipped  
22 with 3D pixel sensor modules in the innermost layer (L0). The pixel cell dimensions will be either  
23  $25 \times 100 \mu\text{m}^2$  (barrel) or  $50 \times 50 \mu\text{m}^2$  (endcap), with one read-out electrode at the centre of a pixel  
24 and four bias electrodes at the corners. Sensors from pre-production wafers ( $50 \times 50 \mu\text{m}^2$ ) produced  
25 by FBK have been bump bonded to ITkPixV1.1 chip at IZM. Bare modules have been assembled  
26 in Genoa on Single Chip Cards and characterized in laboratory and at test beam.

27 **KEYWORDS:** Hybrid detectors; Radiation-hard detectors; Particle tracking detectors (Solid-state  
28 detectors); Detector design and construction technologies and materials

---

<sup>1</sup>Corresponding author.



---

## 29 Contents

30	<b>1 Introduction</b>	<b>1</b>
31	<b>2 ITk Pixel modules</b>	<b>2</b>
32	2.1 3D sensor	3
33	2.2 ITkPixV1.1 chip	4
34	<b>3 Samples</b>	<b>4</b>
35	3.1 Laboratory test	5
36	3.1.1 Sensor IV	5
37	3.1.2 Threshold tuning	5
38	3.1.3 X-ray data taking	5
39	3.2 Beam test	6
40	3.2.1 Resolution	7
41	3.2.2 Efficiency	7
42	<b>4 Conclusion</b>	<b>8</b>

---

## 43 1 Introduction

44 In the next years, the Large Hadron Collider (LHC) will be upgraded (High Luminosity LHC [1])  
45 to reach higher instantaneous luminosity, up to  $7.5 \cdot 10^{34} \text{ cm}^{-2} \text{ s}^{-1}$ . To cope with the higher particle  
46 rate, hit occupancy and radiation damage, the ATLAS detector [2] will be updated as well: in  
47 particular, its tracking system will be completely replaced by a new all-silicon detector (Inner  
48 Tracker, ITk), to be installed during the Long Shutdown 3 (2026-2028). ITk will consist of a Pixel  
49 detector [3] at small radius and a large area Strip detector [4] surrounding it. In particular, the  
50 innermost layer (L0) of the Pixel detector will face a non ionising fluence up to  $2 \cdot 10^{16} \text{ n}_{eq}/\text{cm}^2$  and  
51 a ionising dose up to 1 Grad.

52 After several years of R&D [5], 3D sensors were chosen for the L0 pixel modules, with a square  
53 pixel cell ( $50 \times 50 \mu\text{m}^2$ ) in the endcap rings modules and a rectangular pixel cell ( $25 \times 100 \mu\text{m}^2$ ) in  
54 the barrel ones. 3D sensors diced from previous batches of wafers produced by FBK (Fondazione  
55 Bruno Kessler) [6–8] were bonded to the FE-I4 [9] or RD53A [10] readout chips: these prototype  
56 modules were characterized in laboratory and beam test [11, 12] up to a fluence of  $1 \cdot 10^{16} \text{ n}_{eq}/\text{cm}^2$ .  
57 The results collected on prototypes have demonstrated the validity of the technology in the ITk  
58 detector conditions: to move forward, pre-production has been launched.

59 In this paper, we report on the characterization of the modules assembled with the first pre-  
60 production 3D sensors produced by FBK bonded to ITkPixV1.1 chips, including laboratory char-  
61 acterization and beam test results of unirradiated samples.

62 **2 ITk Pixel modules**

63 The latest ITk Pixel detector layout [13] includes 5 layers of pixel in the barrel and several disks  
 64 in the endcap. The two innermost layers (L0 and L1 barrel layers, together with R0, R0.5 and R1  
 65 rings) will make up the Inner System (see Figure 1), which is planned to be replaced after about  
 66  $2000 \text{ fb}^{-1}$ . Hybrid pixel modules will be glued to carbon support structures. Quad-modules (one  
 67 bare module, with four chips bonded to a planar sensor, glued to a flexible PCB) will be hosted in  
 68 the external layers (L1-4):  $150 \mu\text{m}$  planar sensors in L2-4 (Outer Barrel and Outer Endcap), while  
 69  $100 \mu\text{m}$  planar sensors in L1, R1 and R0 (Inner System, Figure 2, left).

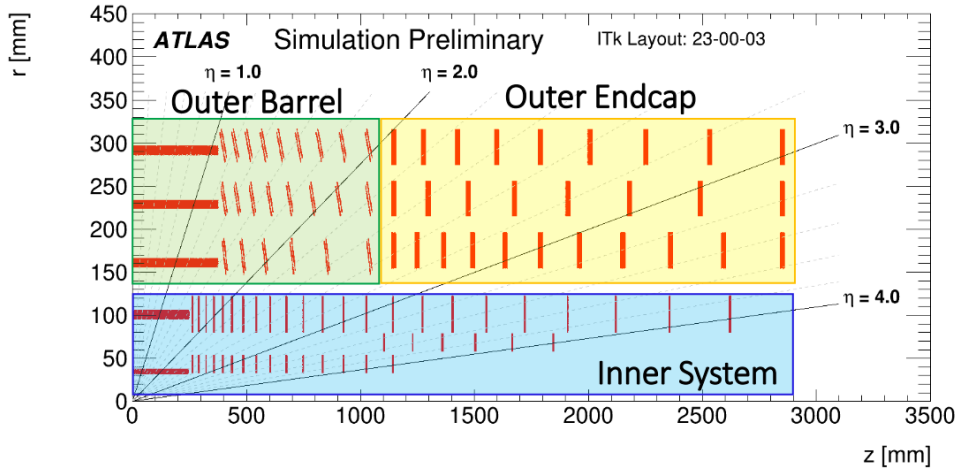


**Figure 1.** ITk Pixel detector layout, 3 sub-sections outlined: Outer Barrel, Outer Endcap and Inner System.

70 Triplet modules (three separate bare modules, each with a 3D sensor bonded to a chip, glued  
 71 to a flexible PCB) will be at 34 mm from collisions (L0) in the barrel or down to 33.2 mm (R0) in  
 72 the endcap (Figure 2, left). A total of 288 (900) 3D sensors are needed to equip the triplet modules  
 73 in the barrel (rings). In particular, there will be 12 L0 staves (barrel) with 8 triplets each, and two  
 74 type of rings (endcap): 30 R0 rings, with 6 triplet modules and 20 planar modules each, and 12  
 75 R0.5 rings with 10 triplet modules each. The number of carbon supports, triplet modules and 3D  
 76 sensors needed is summarized in Table 1.

**Table 1.** Number of carbon supports, triplet modules and 3D sensors in the ITk detector.

	Supports	Triplets per support	Total triplets	Total 3D sensors	Pixel cell [ $\mu\text{m}^2$ ]
L0	12 staves	8	96	288	$25 \times 100$
R0	30 rings	6	180	540	$50 \times 50$
R0.5	12 rings	10	120	360	$50 \times 50$

77 The ITk detector project just completed the prototyping phase: prototype carbon supports  
 78 equipped with services and RD53A modules have been built and tested. A R0 ring prototype  
 79 equipped with RD53A modules can be seen in Figure 2, right. The community is now moving  
 80 towards the detector production: an intermediate step, the pre-production, is currently ongoing.  
 81 Details about pre-production of FBK 3D sensors and ITkPixV1.1 chips are given below.

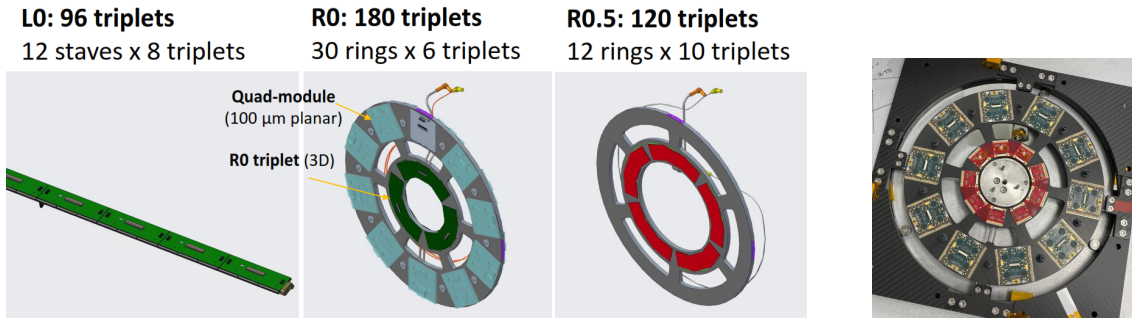


**Figure 2.** Left: L0, R0 and R0.5 supports for triplet modules. Right: Prototype of R0 ring carbon support with RD53A modules, one side loaded with 10 quad-modules and 3 triplets.

82 **2.1 3D sensor**

83 Pre-production 3D sensors are being produced by FBK, SINTEF and CNM foundries. The sensors  
 84 of interest for this report ( $50 \times 50 \mu\text{m}^2$ ) have been produced on 6 inches wafer (24 sensor each,  
 85 Figure 3, left) designed at the University of Trento and fabricated at FBK (Trento, Italy). The  
 86 3D pixel is built in single-sided technology with columns etched in a  $150 \mu\text{m}$  active layer (high-  
 87 resistivity  $p^-$ ), bonded to a  $500\text{-}\mu\text{m}$  thick low-resistivity ( $p^{++}$ ) handle wafer (Figure 3, right). The  
 88 handle wafer is thinned to  $\sim 100 \mu\text{m}$  after dicing and before flip-chip bonding to the readout chip.  
 89 The ohmic ( $p^+$ ) columns pass through the active layer and penetrate the handle wafer to facilitate  
 90 the bias from the backside. The readout ( $n^+$ ) columns stop about  $\sim 20 \mu\text{m}$  before the end of the  
 91 active layer. A p-spray layer (not shown in the Figure) isolates the  $n^+$  columns at the surface. The  
 92  $n^+$  column is connected to the bump pad through a contact, these surface details can be seen in  
 93 Figure 4: left, the layout of the cell and right, photo of the surface of a pre-production wafer pixel  
 94 cell.

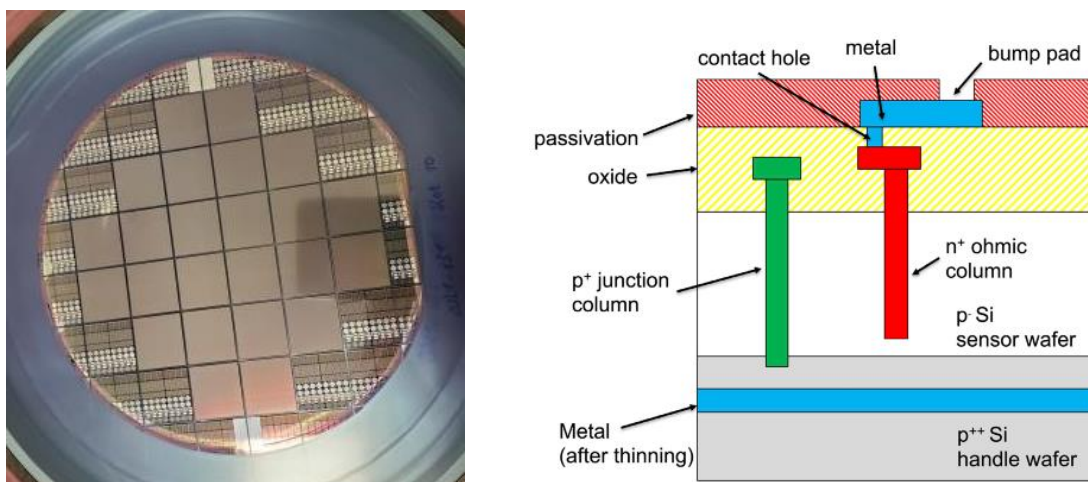


**Figure 3.** Left: six inches FBK pre-production wafer with 24 sensors (and test structures at the periphery). Right: schematic cross section of 3D pixel sensor built in single-side technology.

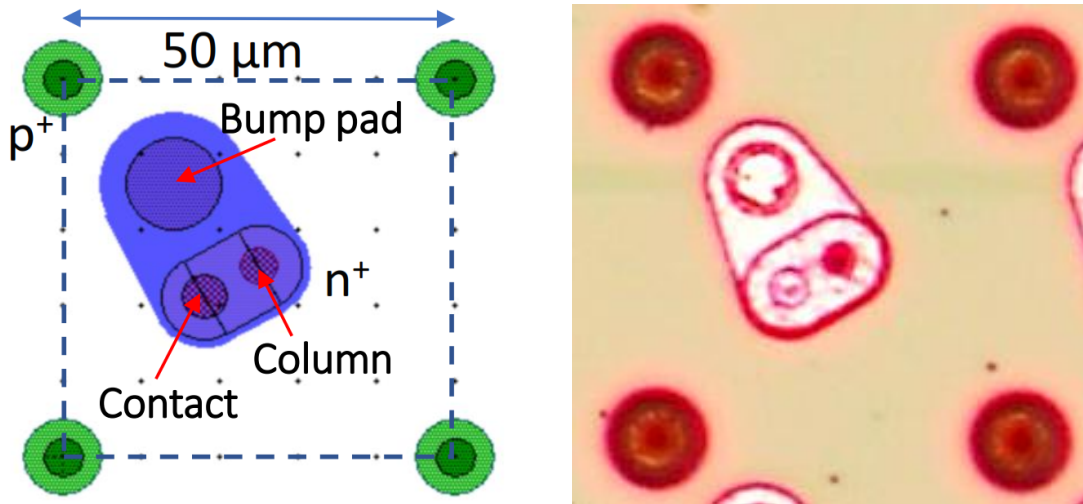


**Figure 4.** Left: 3D pixel cell layout. Right: surface of a pixel cell from FBK pre-production wafer. The bump pad observed in wafer is smaller due to an error in the in the pre-production layout, that was fixed later.

## 95 2.2 ITkPixV1.1 chip

96 After the positive experience gained by testing planar and 3D sensor modules with RD53A chip, a  
 97 new common library has been prepared, so-called RD53B [14], to develop the final layout of the  
 98 ATLAS (ITkPixV1) and CMS (CROC v1) readout chips. The first version of the ATLAS chip,  
 99 ITkPixV1.0, was submitted in March 2020. This very first version presented a problem with Time  
 100 over Threshold (ToT), which caused a significant increase in current and made it impossible to use  
 101 for data taking. An updated version, ITkPixV1.1, was submitted in 2021: the issue with the ToT  
 102 has been overcome by disabling it with simple changes in the more external wafer layer.

103 Several ITkPixV1.1 wafers were produced, probed, thinned (to 150 μm) and diced: a 80%  
 104 green yield is achieved. ITkPixV1.1 is still a prototype, the final version of the chip, ITkPixV2,  
 105 will be submitted at the end of 2022.

106 ITkPixV1 chip has a matrix of 50×50 μm<sup>2</sup> pixels, with 384 rows and 400 columns. A total  
 107 area of about 2×2 cm<sup>2</sup>, with a power dissipation of about 0.5 W/cm<sup>2</sup>. The discrimination threshold  
 108 can be set to 1000 *e* (target value), but it is possible to tune to lower values: 600 *e* without noisy  
 109 pixels, 400 *e* with 1% noisy pixels. The properties of ITkPixV1 chip have been studied in depth,  
 110 also with irradiation up to 1 Grad [15].

## 111 3 Samples

112 Five pre-production wafers have been delivered by FBK to CERN in 2021. Among them, 20  
 113 sensors were diced out and flip-chipped at IZM to ITkPixV1.1 chips: these early modules have been  
 114 tested for sensor pre-production quality assessment. Six of these modules have been assembled  
 115 in Genoa on dedicated PCBs that host a single module/chip: Single Chip Cards (SCCs). Tests  
 116 executed in INFN Genoa laboratory on the six samples are documented in section 3.1, while results  
 117 of measurements performed at CERN beam facilities on SCC 2 and 4 are described in section 3.2.

### 118 3.1 Laboratory test

119 The tests executed in INFN Genoa laboratory includes: sensor IV, chip threshold tuning and data  
120 acquisition with X-rays.

#### 121 3.1.1 Sensor IV

122 Sensor IV was previously measured at sensor level (on wafer) in Trento, then on bare module  
123 (assembled on SCC) in Genoa. Measurements at room temperature are performed up to 80 V bias,  
124 then scaled to 20°C for comparison. For all the six samples, the leakage current at 25 V (20 V  
125 higher than the depletion voltage, assumed to be around 5 V) is always below  $0.05 \mu\text{A}/\text{cm}^2$ , much  
126 lower than the technical requirement:  $2.5 \mu\text{A}/\text{cm}^2$ . The results obtained on wafer (red) and on SCC  
127 (blue) for one of the samples assembled in Genoa can be seen in Figure 5. The minor increase of the  
128 leakage current at bare module level is not considered worrisome, it may be due to the hybridization  
129 steps (wafer dicing, flip-chip).

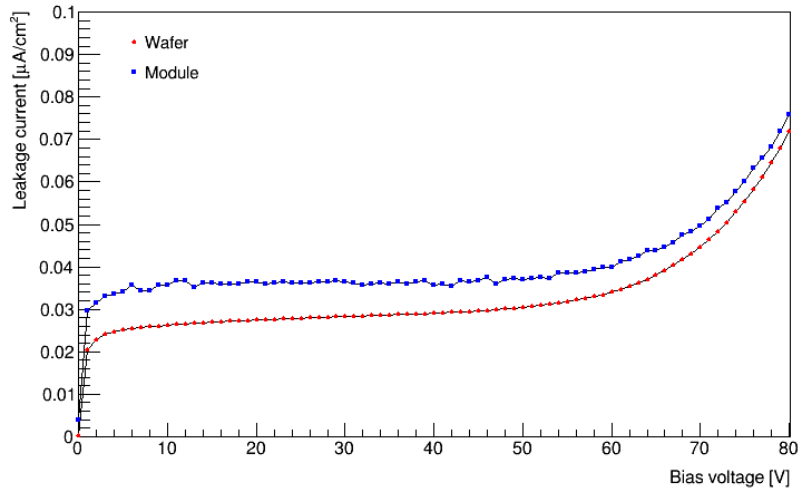


**Figure 5.** IV measured on the same sensor directly on wafer (red) and on bare module mounted on SCC 8 (blue). Room temperature measurements: the leakage current values have been scaled to 20°C.

#### 130 3.1.2 Threshold tuning

131 The threshold tuning has been executed with a YARR DAQ system [16] with sensor bias of 10 V.  
132 The target threshold was set to 1000  $e$ : an homogeneous distribution was achieved on all samples,  
133 with a threshold dispersion of about 30  $e$ . The corresponding noise was observed to be  $\sim 70 e$  on  
134 modules with sensor (10 V bias), to be compared to  $\sim 40 e$  observed on bare chip. As expected,  
135 the noise decreases by increasing the bias voltage (Figure 6): it reaches a plateau at about 6 V: this  
136 suggests that the sensor is completely depleted at this bias voltage.

#### 137 3.1.3 X-ray data taking

138 A 60 second long self-trigger scan with X-rays from Amptek Mini-X2 is performed to qualify the  
139 data acquisition capability. In these conditions (tube powered at 50 kV and 80  $\mu\text{A}$ , with the tip at  
140 15 cm from the module), about 6700 hits/pixel in 60 seconds (110/pixel/s) are collected by the inner

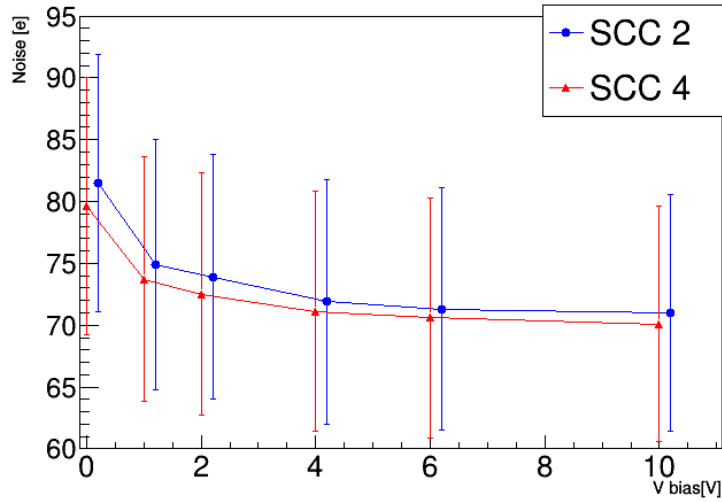


**Figure 6.** Threshold noise decreasing versus bias voltage: a plateau is reached at about 6 V. The standard deviation of the threshold noise distribution is reported as the uncertainty.

141 pixels of the matrix (Figure 7, left), while the edges pixels, both horizontal and vertical, recorded  
 142 about 30% more hits (Figure 7, left). This is explained by the fact that the electric field that collects  
 143 the charge in the edges pixels extends partly also in the slim edge region of the sensor (Figure 7,  
 144 left).

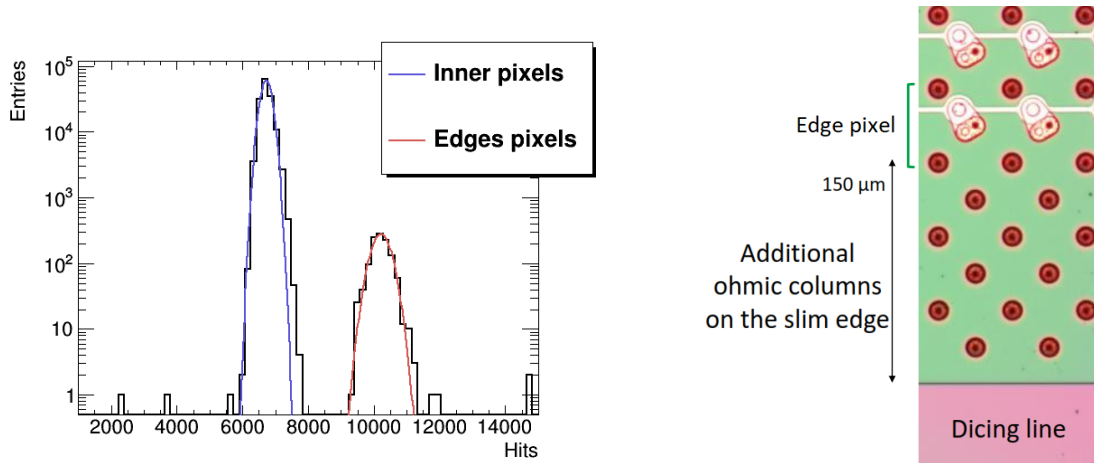


**Figure 7.** Left: Hit occupancy with 60 s long X-ray scan. Right: edges pixel cells, with 150  $\mu\text{m}$  of additional ohmic columns before the dicing line.

### 145 3.2 Beam test

146 During Spring 2022, two test beam campaigns have been performed to study the performance of the  
 147 unirradiated modules on the beam. The first campaign took place at the PS (12 GeV protons), then  
 148 the setup was moved to the SPS (about 120 GeV pions). The setup included a telescope with six  
 149 MIMOSA26 [17] planes and a FE-I4 chip module as a timing reference plane. The data acquisition

150 system was YARR and EUDAQ based. The coincidences of two scintillators, placed at the two ends  
 151 of the telescope, were used to generate the trigger signal for the readout, distributed to telescope  
 152 planes and Devices Under Test (DUTs) by a Trigger Logic Unit (TLU).

153 At the PS facility, data were collected supplying the DUT sensor with a bias of 1, 2, 4, 6 and  
 154 10 V, while at SPS data were taken only with a bias of 0 and 10 V. SCC 2 was tested only at the  
 155 PS, while SCC 4 in both facilities. The SCCs, tuned to a 1000 e threshold, were perpendicular  
 156 to the beam inside an aluminum coldbox. Data have been analyzed using the Corryvreckan [18]  
 157 framework. Data in EUDAQ-native raw format were loaded on Corryvreckan, the noisy pixels were  
 158 masked on each device, then the telescope planes were aligned, followed by the DUTs. Finally, the  
 159 resolution and efficiency of DUTs were measured.

### 160 3.2.1 Resolution

161 Since the ToT reading was disabled for the ITkPixV1.1 chip, only binary read-out is possible.  
 162 Therefore the expected resolution ( $\sigma = \text{pitch}/\sqrt{12}$ ) for the  $50 \times 50 \mu\text{m}^2$  pixel cell is about  $14 \mu\text{m}$  in  
 163 both the X and Y directions. The residuals RMS observed at the SPS is about  $13 \mu\text{m}$ , as expected,  
 164 while at the PS it is higher (20-25  $\mu\text{m}$ ): this could be explained by the lower particle beam energy  
 165 at PS, which increases the multiple scattering due to the aluminum walls of the cooling box.

### 166 3.2.2 Efficiency

167 Several runs were collected for each bias voltage point: for each point, the mean value and the  
 168 standard deviation of the efficiency are extracted by a Gaussian fit to the distribution of the results  
 169 obtained in each run. At PS, the efficiency was always higher than 97%. At SPS, the efficiency is  
 170 already  $(98.6 \pm 0.1)\%$  with a bias voltage of 0 V, reaching  $(98.9 \pm 0.1)\%$  with a bias of 10 V (Figure 8,  
 171 left). The efficiency is almost 100% in the central part of the pixel cell,  $(99.91 \pm 0.02)\%$  at 10 V,  
 172 while in the corner it is lower, down to 75% (Figure 8, right). The inefficiency zone, due to the  
 173  $p^+$  columns (max 4  $\mu\text{m}$  radius), extends for about 10  $\mu\text{m}$  in both 0 and 10 V bias (Figure 9). The  
 174 efficiency in the dead area due to the  $p^+$  columns is expected to be of 0%: the effect is smeared by  
 175 the telescope resolution ( $\sim 5 \mu\text{m}$ ), that likely also makes the size of the region with lower efficiency  
 176 to appear larger than its true value.

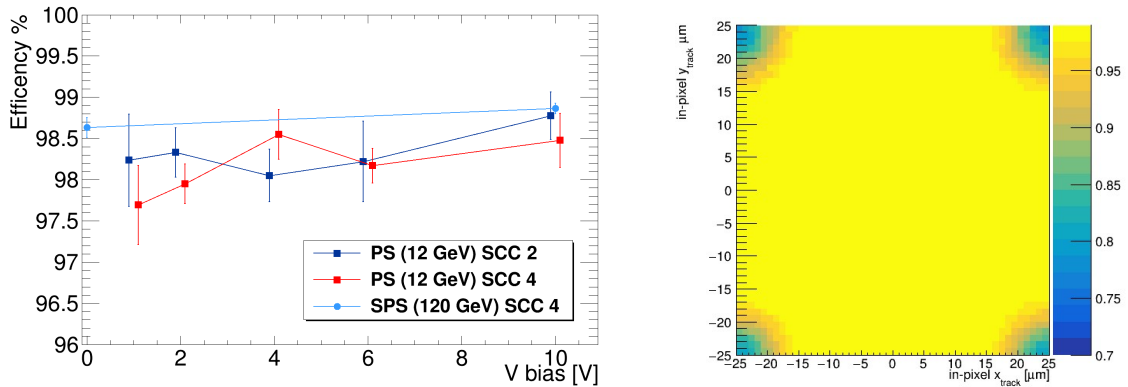


**Figure 8.** Left: Efficiency versus bias voltage at PS and SPS. Right: Pixel cell efficiency at 10 V (SPS data).



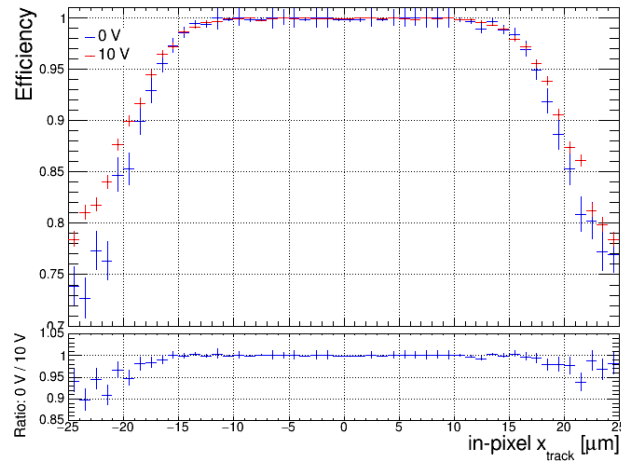


**Figure 9.** Projection of the first  $1 \mu\text{m}$  along the X direction of the pixel local efficiency map at 0 and 10 V bias (SPS data): the inefficiency zone due to the  $p^+$  columns (max  $4 \mu\text{m}$  radius) extends for about  $10 \mu\text{m}$ .

## 177 4 Conclusion

178 ITk detector, the new ATLAS tracking system at High Luminosity LHC, will be equipped with  
 179 3D pixel sensor modules in the innermost layer. Sensors from pre-production wafers produced by  
 180 FBK have been bump bonded to ITkPixv1.1 chip. Bare modules have been assembled in Genoa on  
 181 Single Chip Cards and characterized in laboratory and with beam at CERN facilities.

182 The leakage current is well below  $0.2 \mu\text{A}/\text{cm}^2$  in the considered bias voltage range (0-80 V).  
 183 At 10 V bias, an average noise of  $70 \pm 10 e$  has been observed after tuning the threshold to 1000  $e$ .  
 184 The edges pixels record about 30% more hits than pixels in the center of the matrix, due to the  
 185 extension of the electric field in the slim edge. Hit detection efficiency higher than 97% has been  
 186 measured on modules before irradiation already at 0 V bias.

187 Two devices has been irradiated with protons up to  $1 \cdot 10^{16} n_{eq}/\text{cm}^2$  fluence and 1 Grad dose,  
 188 characterization with the beam is ongoing at SPS.

## 189 Acknowledgments

190 This work was partially funded by the Italian National Institute for Nuclear Physics (INFN), Projects  
 191 RD\_FASE2 and FASE2\_ATLAS (CSN1), and by the H2020 project AIDA-2020, GA No. 654168.  
 192 The test beam measurements were performed at the CERN Test Beam Facility (PS and SPS).

## 193 References

- 194 [1] G. Apollinari *et al.*, *High-Luminosity Large Hadron Collider (HL-LHC): Technical Design Report*,  
 195 CERN Yellow Reports: CERN-2020-010, CERN, Geneva (2020)
- 196 [2] ATLAS Collaboration, *The ATLAS Experiment at the CERN Large Hadron Collider*, *JINST* **3** S08003  
 197 (2008)
- 198 [3] ATLAS collaboration, *ATLAS Inner Tracker Pixel Detector TDR*, Technical Design Report  
 199 *CERN-LHCC-2017-021*, CERN, Geneva (2017)

- 200 [4] ATLAS collaboration, *ATLAS Inner Tracker Strip Detector TDR*, Technical Design Report  
201 *CERN-LHCC-2017-005*, CERN, Geneva (2017)
- 202 [5] S. Terzo *et al.*, *Novel 3D pixel sensors for the upgrade of the ATLAS Inner Tracker*, *Frontiers in*  
203 *Physics* 624688 (2021)
- 204 [6] G.-F. Dalla Betta *et al.*, *Development of a new generation of 3D pixel sensors for HL-LHC Nucl.*  
205 *Instrum. Meth. A* **824** 386-387 (2016)
- 206 [7] D M S Sultan *et al.*, *First Production of New Thin 3D Sensors for HL-LHC at FBK*, *JINST* **12** 01,  
207 C01022 (2017)
- 208 [8] M. Boscardin *et al.*, *Advances in 3D Sensor Technology by Using Stepper Lithography*, *Frontiers in*  
209 *Physics* 625275 (2020)
- 210 [9] M. Garcia-Sciveres *et al.*, *The FE-I4 pixel readout integrated circuit*, *Nucl. Instrum. Meth. A* **636**  
211 S155 (2011)
- 212 [10] M. Garcia-Sciveres *et al.*, *The RD53A Integrated Circuit*, Technical Report  
213 *CERN-RD53-PUB-17-001*, CERN, Geneva (2017)
- 214 [11] H. Oide *et al.*, *INFN-FBK developments of 3D sensors for High-Luminosity LHC*, *Nucl. Instrum.*  
215 *Meth. A* **924** 73-77 (2019)
- 216 [12] Md.A.A. Samy *et al.*, *Characterization of FBK 3D pixel sensor modules based on RD53A readout*  
217 *chip for the ATLAS ITk*, *JINST* **16** C12028 (2021)
- 218 [13] ATLAS collaboration, *Expected tracking and related performance with the updated ITk layout*, Public  
219 note *ATL-PHYS-PUB-2021-024*, CERN, Geneva (2021)
- 220 [14] M. Garcia-Sciveres *et al.*, *RD53B Manual*, Technical Report *CERN-RD53-PUB-19-002*, CERN,  
221 Geneva (2019)
- 222 [15] M. Mironova, *Measurements of the radiation damage to the ITkPixV1 chip in X-ray irradiations*,  
223 *Nucl. Instrum. Meth. A* vol **1039** 166947 (2022)
- 224 [16] T. Heim, *YARR - A PCIe based Readout Concept for Current and Future ATLAS Pixel Modules*, *J.*  
225 *Phys.: Conf. Ser.* **898** 3 032053 (2017)
- 226 [17] C. Hu-Go *et al.* *A ten thousand frames per second readout MAPS for the EUDET beam telescope.*,  
227 *Proceedings TWEPP09* (2009)
- 228 [18] J. Kröger *et al.* *User Manual for the Corryvreckan Test Beam Data Reconstruction Framework*,  
229 *Version 1.0*. arXiv:1912.00856 (2019)